The Momentum Turbulent Counter–Gradient Transport in Jet–like Flows

V. N. Lykossov

Institute of Numerical Mathematics, USSR Academy of Sciences, Moscow, USSR

Received May 22, 1991; revised September 7, 1991

I. INTRODUCTION

It is very well known from the observations that some atmospheric motions are accompanied by jets in the boundary layer, for example, breezes and circulations in the mountain valleys (Gutman, 1969); nocturnal increasing of wind (Byzova et al., 1989); cross–equatorial flow during the summer Indian monsoon (Das, 1986) and others. One of the important questions concerning a mathematical modelling of such motions is the problem of the turbulent closure of the equations set which describes the jet dynamics. It is still popular to use for the momentum turbulent flow $(\overline{u'w'})$ a closure, based within the framework of K–theory on the Boussinesq hypothesis

$$\overline{u'w'} = -K\frac{\partial \overline{u}}{\partial z} , \tag{1}$$

where z is the vertically directed upwards coordinate; u, w–horizontal and vertical components of wind velocity; K–eddy exchange coefficient (due to physical meaning positive one); averages are denoted by overbars, and fluctuating quantities by primes. But of late years, it was shown that relationship (1) has some essential shortcomings, which restrict the usage of this formula.

For example, the very interesting case of jet has been observed in the fair–weather trade wind boundary layer to the northeast of Puerto Rico in December 1972 (Pennel and LeMone, 1974; their Fig.4). The maximum of wind velocity was placed near the surface; the negative wind shear area has occupied upper two–thirds of the boundary layer. But at the same time it was found that the direction of momentum transport over the entire boundary layer was toward the surface. It follows, therefore, that in the case of negative wind shear momentum transport is counter–gradient.

Results of the laboratory modelling of the turbulence within a baroclinic mixed layer above a sloping surface, which are presented in the paper of Deardorff and Willis (1987), show, that jet–like flow near the tank bottom is compensated by return flow in the upper part of the boundary layer (Fig.4 of the considered paper). The vertical profile of flux $\overline{u'w'}$, given in Fig.5 of that paper, does not allow to draw any information about counter–gradient diffusion of momentum at the height of the near–bottom velocity maximum, but it bears an evidence of such diffusion in the upper part of the mixed layer (see also Fig.6 of the considered paper, which shows terms of the turbulent kinetic energy balance: shear production is negative above the level of the return flow velocity maximum). It is strange that Deardorff and Willis have not discussed this feature of experimental data. Moreover, their conclusion that momentum flux could be expressed in form (1) is in contradiction with their Fig.6, because in this case the shear production must be non–negative everywhere.

In the Narasimha's survey (1984) of the turbulence in simple flows another example of the laboratory simulated wall–jet is given. Fig.5d of his review shows that in such flow the counter–gradient transport of momentum was observed just below velocity maximum height. The same features of the wall boundary layer with jet–like flows were discussed in the work of Wood and Bradshaw, 1984 (see Figs.2 and 6 of their paper).

Finally, the numerical simulation of the atmsopheric boundary layer vertical structure over the curved underlying surface in presence of horizontal heat advection (Speranskiy et al., 1974) has shown that even if formation of nocturnal jet was caused by the coupled effect of baroclinicity and topography, intensity of jet depended very much on the character of the momentum turbulent transport mechanism.

Let us consider this in more detail. We can write the equation for the time () change of the averaged velocity $\overline{u}$ as follows

$$\frac{\partial \overline{u}}{\partial t} = -\frac{\partial}{\partial z}(\overline{u'w'}) + \cdots\cdots , \tag{2}$$

where dots denote terms describing the input of other physical processes into jet dynamics. Let us assume for the definition that $\overline{u} > 0$. Introducing the relation (1) into formula (2) we get

$$\frac{\partial \overline{u}}{\partial t} = \frac{\partial K}{\partial z}\frac{\partial \overline{u}}{\partial z} + K\frac{\partial^2 \overline{u}}{\partial z^2} + \cdots\cdots \tag{3}$$

At the jet axis we have $\frac{\partial \overline{u}}{\partial z} = 0$, $\frac{\partial^2 \overline{u}}{\partial z^2} < 0$ and therefore the parameterization of the momentum turbulent flux in Boussinesq form (1) leads us to the systematic decay of the (simulated) velocity maximum.

In the author's previous paper (Lykossov, 1990) on the basis of the second moments equations it was found in the quasi–stationary approximation that the Boussinesq hypothesis can be generalized as follows

$$\overline{u'w'} = -K\left[\frac{\partial \overline{u}}{\partial z} - \gamma_u\right] , \tag{4}$$

where γ_u is so–called counter–gradient, which in commom case depends on the wind shear, Brunt–Vaisala's frequency, turbulent frequency (relaxation time) and some combination of third–order convariances. Introducing the expression (4) into formula (2) we get following relationship

$$\frac{\partial \overline{u}}{\partial t} = \frac{\partial K}{\partial z}\frac{\partial \overline{u}}{\partial z} + K\frac{\partial^2 \overline{u}}{\partial z^2} - \frac{\partial}{\partial z}\left[K\gamma_u\right] + \cdots\cdots \tag{5}$$

from which one can see that in some cases the dissipative effect of the velocity profile curvature at the jet axis can be compensated by non–local (counter–gradient) turbulent transprot of the momentum. In the above mentioned paper of Speranskiy et al. (1974) it was taken that $\gamma_u = \partial u_g / \partial z \equiv \text{const}$, where u_g is geostrophic wind velocity. Considered in that paper the situation was characterized by $\gamma_u > 0$ and $\partial K / \partial z < 0$ in the jet area. These conditions gave a possibility to "support" jet in the model calculations.

Modern high–order–closure models, eddy–resolvable models and calculations of the turbulent statistics, based on the direct measurements of meteorological parameters in the atmospheric boundary layer, allow, in principle, to estimate conditions, when momemtum transport under consideration in low–level jets can take place. But such models require for their realization large computer resources. Higher order statistics calculations are demanding a fine accuracy of the direct measurements. In connection with this, simplified models reflecting main features of the problem under consideration, are useful.

II. PROBLEM FORMULATION

In the present work we neglect effects of thermal stratification, assume that vertical profiles of horizontal averaged wind velocity ($\bar{u}$), vertical velocity dispersion ($\overline{w'^2}$) and turbulent frequency ($\omega = e^{1/2}/l$, where e is the turbulent kinetic energy, l turbulence length) are known. We consider the problem in the stationary and horizontally homogeneous approximation. Then equations for the second and third covariances can be extracted from third–order–closure model (Andre, 1976; Moeng and Randall, 1984; Kurbazkiy, 1988) and are as follows

$$\frac{d}{dz}(\overline{u'w'^2}) + \overline{w'^2}\frac{d\bar{u}}{dz} + C_1 C_4 \omega \overline{u'w'} = 0 \ , \tag{6}$$

$$2\overline{w'^2}\frac{d}{dz}(\overline{u'w'}) + \overline{u'w'}\frac{d}{dz}(\overline{w'^2}) + (1 - C_{11})\overline{w'^3}\frac{d\bar{u}}{dz} + C_1 C_8 \omega \overline{u'w'^2} = 0 \ , \tag{7}$$

$$3\overline{w'^2}\frac{d}{dz}(\overline{w'^2}) + C_1 C_8 \omega \overline{w'^3} = 0 \ . \tag{8}$$

In Eqs.(6)–(8) the variable $\overline{u'w'^2}$ stands for the vertical turbulent diffusion of the momentum flux; function $\overline{w'^3}$ describes the vertical flux of the dispersion $\overline{w'^2}$; parameters C_1, C_4, C_8 and C_{11} are "universal" constants.

These constants have a following meaning: C_1 is the proportionality coefficient in the well known Kolmogoroff's (1942) relationship between the dissipation rate, turbulent kinetic energy and turbulence length; C_4 is parameter in Rotta (1951) formula, giving proportionality between pressure gradient / velocity covariance and momentum; C_8 and C_{11} are link coefficients between 3rd order covariance pressure gradient / energy and momentum flux components and gradient of the averaged velocity in the "relaxation approximation" hypothesis (Kurbazkiy, 1988; Moeng and Randall, 1984). Besides relationships mentioned according to Milliontschikov's (1941) hypothesis of quasinormal approximation, which allows to express 4th order covariances through covariances of 2nd order, has been used in Eqs.(7) and (8).

In the momentum balance Eq.(6) the first term characterizes the turbulent trnasport of momentum $\overline{u'w'}$; the second one describes the momentum generation due to interaction between mean flow and fluctuating flow; the last one is the result of Rotta (1951) parameterization for the interactions between fluctuations of pressure and velocity. The following Eq.(7) is the balance equation for the "flux of momentum flux" and in this equation first two terms, which are equivalent, due to Milliontschikov's (1941) hypothesis, to the gradient of the 4th order covariance $\overline{u'w'^3}$, describe the turbulent diffusion of the $\overline{u'w'^2}$. The third term of this equation consists of two parts, first of which characterizes the generation of the covariance $\overline{u'w'^2}$ due to interaction between mean and fluctuating flow and second one together with last term of Eq.(7) is result of " relaxation approximation" hypothesis (Kurbazkiy, 1988; Moeng and Randall, 1984) application.

Similarly, in the Eq.(8), which is the balance of the vertical dispersion flux, first term describes its turbulent diffusion $\frac{d\overline{w'^4}}{dz}$ and the second one is the consequence of the application of the "relaxation approximation" relationship.

In the considered formulation Eq.(8) is an algebraic relationship. Therefore, we can formulate only two boundary conditions, which we chose as follows:

$$\overline{u'w'} = \tau_0 \qquad \text{for } z = 0 \tag{9}$$

$$\overline{u'w'} \to 0 \qquad \text{for } z \to \infty \tag{10}$$

where τ_0 is a known momentum flux value at the surface.

Equations set (6)–(8) by simple transformations can be reduced to one ordinary differential equation of 2nd order for $\overline{u'w'}$

$$\frac{d}{dz}\left[v\frac{d}{dz}(\overline{u'w'})\right] + \frac{d}{dz}\left[\mu\overline{u'w'}\right] + \alpha\omega\overline{u'w'} = \beta_1\omega v\frac{d\bar{u}}{dz} + \beta_2\frac{d}{dz}\left[\mu v\frac{d\bar{u}}{dz}\right], \tag{11}$$

where it is denoted:

$$v = \omega^{-1}\overline{w'^2}, \quad \mu = (1/2)\omega^{-1}\frac{d}{dz}(\overline{w'^2}) .$$

$$\alpha = (1/2)C_1^2C_4C_8, \quad \beta_1 = (1/2)C_1C_8, \quad \beta_2 = 3(1 - C_{11})C_1C_8 . \tag{12}$$

J[65] Using values of constants, given in the Moeng and Randall (1984) paper,

$$C_1 = 0.07; \quad C_4 = 4.5; \quad C_8 = 8.0; \quad C_{11} = 0.2,$$

we get

$$\alpha = 0.09; \quad \beta_1 = 0.28; \quad \beta_2 = 4.29 .$$

III. QUALITATIVE ANALYSIS

Let us neglect for some time the first two terms in the left–hand side of Eq.(11). Then this equation takes up the form of generalized Boussinesq hypothesis (4) with

$$K = \alpha^{-1}\beta_1 v, \quad \gamma_u = -\beta_2\beta_1^{-1}\omega^{-1}v^{-1}\frac{d}{dz}\left[\mu v\frac{d\bar{u}}{dz}\right] . \tag{13}$$

We can rewrite the expression for $\overline{u'w'}$ in a slightly different way

$$\overline{u'w'} = \tau_g + \tau_{cg} , \tag{14}$$

where

$$\tau_g = -K\left\{1 + (1/2)\beta_2\beta_1^{-1}\omega^{-1}v^{-1}\left[\frac{d}{dz}(\mu v) + \left|\frac{d}{dz}(\mu v)\right|\right]\frac{d\bar{u}}{dz}\right\} \tag{15}$$

$$\tau_{cg} = -\beta_2\alpha^{-1}\omega^{-1}\mu v\frac{d^2\bar{u}}{dz^2} - (1/2)\beta_2\beta_1^{-1}\omega^{-1}v^{-1}K\left\{\frac{d}{dz}(\mu v) - \left|\frac{d}{dz}(\mu v)\right|\right\}\frac{d\bar{u}}{dz} . \tag{16}$$

It is possible to see from the formulae (15) and (16), that a component τ_g describes the gradient diffusion of the momentum, and τ_{cg} the possible counter–gradient transport. This possibility of the counter–gradient diffusion depends on interrelationships between τ_g and τ_{cg}. The counter–gradient flux of the momentum takes place, if firstly, signs of τ_g and τ_{cg} are different and, secondly, τ_{cg} is greater on absolute value than τ_g. Taking into account the relation (12) and the turbulent frequency ω definition, we have at the jet axis

$$\tau_g = 0$$

$$\tau_{cg} = (1/2)\alpha^{-1}\beta_2\overline{w'^2}l^3/e^{3/2}\left[\frac{d}{dz}(\overline{w'^2})\right]\frac{d^2\bar{u}}{dz^2} . \tag{17}$$

It is clear that the second formula in (17) is approximately also valid in some neighbourhood of the wind velocity maximum level.

Measurements of the atmospheric wind in trade boundary layer near Puerto Rico (Pennel and LeMone, 1974, Figs.4 and 5) show that practically in the whole mixed layer $d^2\bar{u}/dz^2 < 0$ and the variable $\overline{w'^2}$ is approximately constant below wind velocity maximum level and it is decreasing along height above this level. In lower one–third of the boundary layer $d\bar{u}/dz \geqslant 0$, $\tau_{cg} \leqq 0$ and momentum flux is "classically" toward the surface. In the upper part of the mixed layer $d\bar{u}/dz \leqslant 0$, but also $\tau_{cg} \geqslant 0$ and, therefore, counter–gradient flux of momentum (also toward the surface) is possible if absolute value of γ_u is greater than absolute value of $d\bar{u}/dz$. In the considered case this situation takes place, of course, at the jet axis and in some neighbourhood below. Due to second relationships (17) τ_{cg} is proportional to cube of turbulence length. It means that large eddies play a very important role in the formulation of the momentum counter–gradient transport and in this particular case it is supported by observed data (Pennel and LeMone, 1974, Fig.7).

In the study of Deardorff and Willis (1987) measurements were not conducted in a thin layer below level of near–the–surface velocity maximum. Data for return flow (Fig.5 of Deardorff and Willis' (1987) paper) show that counter–gradient diffusion of the momentum in the upper part of mixed layer can be explained similar to the above considered case.

Unfortunately, in Narasimha's (1984) publication the distribution of $\overline{w'^2}$ is not given. But in this case we can also try to use formulae (17) for the explanation of the momentum counter–gradient diffusion. As one can see from Fig.5d, given in considered review, momentum flux at the jet axis is positive and comparable in absolute values with surface stress τ_0. Because the velocity profile has a negative curvature at the jet axis, one can see from (17), that in this case vertical velocity dispersion must increase along height $\left[\frac{d}{dz}(\overline{w'^2}) > 0\right]$. This conclusion is supported by laboratory modelling data presented in the paper of Wood and Bradshaw, 1984 (Fig.4b of that paper). Because of $\overline{u'w'}$ profile continuity counter–gradient transport must also take place in some neighbourhood below velocity maximum level. The size of this neighbourhood depends on parameters of the formulae (17), the most important of which is obviously turbulence length.

IV. NUMERICAL EXPERIMENTS

The solution of the full problem (Eq.(11) with boundary conditions (9), (10)) has been obtained numerically. For this purpose the finite–difference grid on vertical coordinate z with homogeneous step Δz has been used. Eq.(11) has been approximated by finite–difference one and for the solution of which the factorization method (Marchuk, 1980) was used. Two basic series of numerical experiments have been carried out, in both of which the flow velocity profile was taken as an analytical function

$$\frac{\bar{u}}{\bar{u}_{max}} = \frac{z}{H_j}\exp\left[1 - \frac{z}{H_j}\right], \tag{18}$$

where $\bar{u}_{max}$ is wind velocity value at the jet axis, placed at height H_j.

In the first series of experiments the profile of the vertical velocity dispersion $\overline{w'^2}$ was chosen as monotonous decreasing along height function

$$\frac{\overline{w'^2}}{\overline{w'^2}_{max}} = \exp\left[-\frac{z}{H_*}\right], \tag{19}$$

where H_* is some vertical scale and $\overline{w'^2}_{max}$ the maximum value of $\overline{w'^2}$. In the second series of experiments the function $\overline{w'^2}$ was taken as the distribution, which has a maximum inside the domain at height $H_* > H_j$.

$$\frac{\overline{w'^2}}{\overline{w'^2_{max}}} = (1/2)\left\{1 + \frac{z}{H_*}\exp\left[1 - \frac{z}{H_*}\right]\right\} . \tag{20}$$

In both the series, numerical experiments have been carried out for 3 different values of the turbulence length: $l = 50$, 100 and 200 m. It was assumed that $e = r\overline{w'^2}$ with constant proportionality coefficient r. The height of calculation domain was chosen equal to 1000 m; H_j and H_* were, in all experiments, taken equal to 200 m and 400 m respectively. The step Δz was assumed to be equal to 10 m. Other parameters were not changed either from experiment to experiment and were chosen as follows

$$r = (3/2); \quad \bar{u}_{max} = 5 \text{ m/s}; \quad \overline{w'^2_{max}} = 0.2 \text{ m}^2/\text{s}^2;$$

$$\tau_0 = -0.2 \text{ m}^2/\text{s}^2 . \tag{21}$$

Let us consider some results of calculations. In Fig.1 vertical profiles of momentum flux $\overline{u'w'}$, calculated in the experiments of series I for different values of the turbulence length ($l = 50$ m for Exp.I.1, $l = 100$ m for Exp.I.2 and $l = 200$ m for Exp.I.3) are given. The distribution of averaged velocity $\bar{u}$ is also shown in this figure by heavy solid line. From Fig.1 one can see that $\overline{u'w'}$ profiles show existence of counter–gradient area above jet axis ($z = 200$ m) in all of three experiments and size of this area depends on the turbulence length value: in Exp.I.1 it is equal to 150 m, in Exp.I.2–350 m and in Exp.I.3 momentum flux is towards the surface in the whole boundary layer.

Estimation (17) shows in this case the cubic dependence of $\overline{u'w'}$ at the wind velocity maximum height (τ_*) on value of lenght l: –0.18, –1.41 and –11.3 m^2/s^2. In numerical experiments an inclusion of the turbulent diffusion (with diffusion coefficient ν) and turbulent advection (with velocity μ) lead to an approximately linear dependence of τ_* on l(–0.35, –0.79 and –1.73 m^2/s^2, respectively). On the whole, Fig.1 reflects qualitatively the main features of $\overline{u'w'}$ distributions, found in the publications of Pennel and LeMone (1974) and Deardorff and Willis (1987). It is also seen from Fig.1, that momentum profiles clearly expressed maxima in the layer, placed below the jet axis. The same feature of $\overline{u'w'}$ can be seen from Fig.6 of Pennel and LeMone's (1974) paper.

Given in Fig.2 are profiles, obtained in the experiments of series II. In these experiments also there exists counter–gradient area; it is placed below the jet axis and its size depends, as in the previous case, on scale l, varying from 60 m in Exp.II.1 to practically whole depth of the layer, placed below the velocity maximum level. At the jet axis an estimation (17) gave following values of τ_*: 0.10 m^2/s^2 in Exp.II.1, 0.78 m^2/s^2 in Exp.II.2 and 6.26 m^2/s^2 in Exp.II.3, but from Fig.2 one can see, that taking into account diffusion and advection we obtained for τ_*: 0.11, 0.62 and 1.74 m^2/s^2 respectively. In contradistinction to the previous case, results of these experiments showed the absence of the linear dependence of τ_* on l. Finishing the discussion of Fig.2 we can say that this figure reflects qualitatively the character of the momentum turbulent transport, denoted in Narasimha's survey (1984) and in the paper of Wood and Bradshaw (1984).

In the previous section we stressed out the important role of the averaged velocity profile curvature in the formation of the momentum counter–gradient diffusion. We have also conducted the experiments, in which parameter β_2 was chosen to be 0, and therefore, curvature effect of $\bar{u}$ distribution was "switched off" in Eq.(11). Results of $\overline{u'w'}$ calculations are presented in Fig.3 (Exp.I.4–I.6 for the same range of parameter l (as in Fig.1) and in Fig.4 (Exp.II.4–II.6 respectively). The level of wind velocity maximum is denoted in these figures by the arrow. From Fig.3 one can see that as in experiments of series I there is

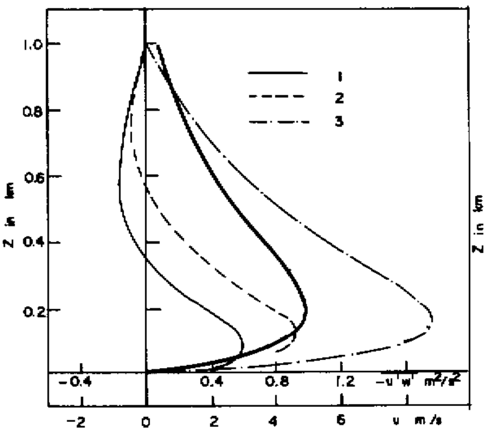

Fig.1. Vertical profiles of momemtum $\overline{u'w'}$, computed in Exp.'s I.1–I.3. By the heavy solid curve the profile of the mean velocity $\bar{u}$, calculated from formula (18) is shown. Distribution of $\overline{w'^2}$ is taken from formula (19).

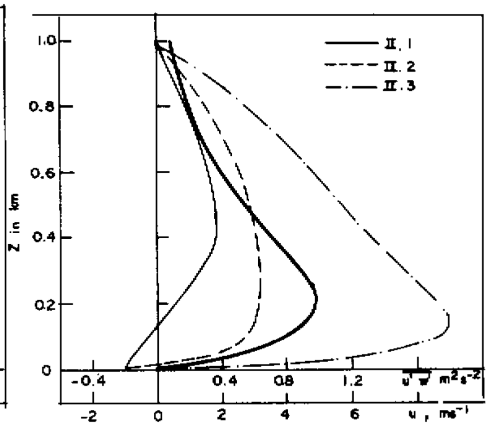

Fig.2. As in Fig.1 but for Exp.'s II.1–II.3. Distribution of $\overline{w'^2}$ is taken from formula (20).

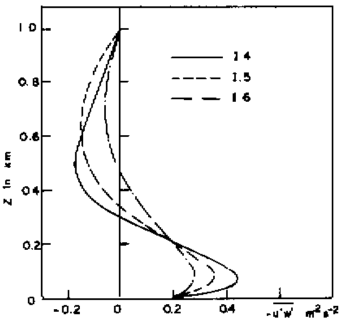

Fig.3. Vertical profiles of momentum $\overline{u'w'}$, computed in Exp.'s I.4–I.6. Parameter β_2 in Eq.(11) is equal to 0.

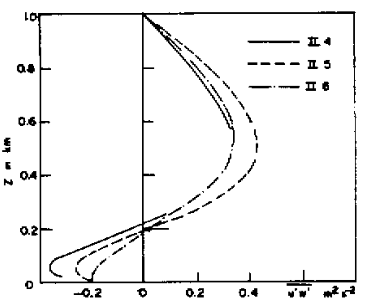

Fig.4. As in Fig.3 but for Exp.'s II.4–II.6.

some counter–gradient area, but its size is now less, than in Fig.1: from 90 m in Exp.I.4 to 250 m in Exp.I.6. Flux $\overline{u'w'}$ is in this case less sensitive to the l variability than in previous experiments I.1–I.3.

A character of $\overline{u'w'}$ transport below the jet axis has totally changed in the experiments of series II, when curvature term in Eq.(11) was "switched off". The counter–gradient area exists, but its size is negligible. Moreover, in Exp.II.4 this area is placed above the wind velocity maximum level. Similar to the series I.4–I.6, dependence of $\overline{u'w'}$ on l is much weaker than it was found from Exp.II.1–II.3 results.

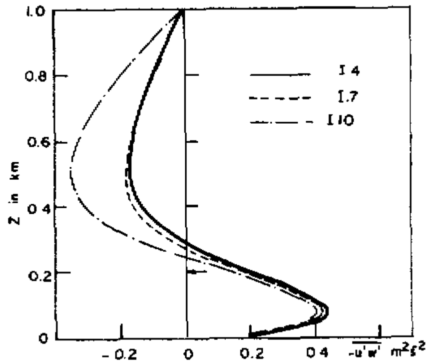

Fig.5. Comparison of $\overline{u'w'}$ profiles calculated in Exp.I.4 ($\beta_2 = 0$, $\mu \not\equiv 0$ in Eq.(11)), Exp.I.7 ($\mu \equiv 0$) and in Exp. I.10 ($\mu \equiv 0$) and in Exp.I.10 ($\mu \equiv 0, \nu \equiv$ const.).

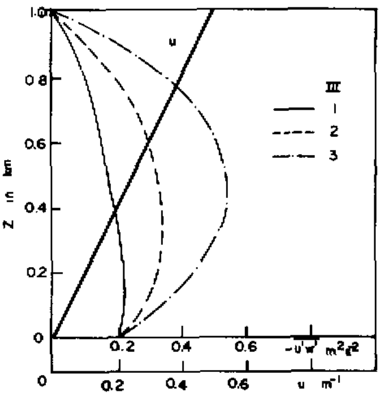

Fig.6. Vertical profiles of momentum $\overline{u'w'}$, computed in Exp.'s III.1–III.3. By heavy solid line the profile of the mean velocity $\bar{u}$ is shown.

In order to estimate the role of the turbulent advection with velocity μ (second term in the left–hand side of Eq.(11)) additional experiments I.7–I.9 and II.7–II.9 have been carried out. In these calculations function μ was put 0 both in this term and in the last term of the right–hand side of Eq.(11). Results of these experiments were compared with results of Exp.I.4–I.6 and II.4–II.6 respectively. An example of such comparison is prsented in Fig.5, which shows vertical profiles of $\overline{u'w'}$, calculated for $l = 50$ m in Exp.I.4 (solid line) and I.7 (dashed line). From Fig.5 one can see that the difference of profiles is small (the same is true also for other experiments with different values of l parameter and alternate vertical distribution (20) of $\overline{w'^2}$). It is necessary to note that in second–order–closure models, using Boussinesq hypothesis (1) for the calculation of covariance $\overline{u'w'^2}$ on the basis of $\overline{u'w'}$ gradient, Eq.(6) takes form (11) with $\mu \equiv 0$.

Let us also note that in the above discussed calculations function μ was formally put 0, but coefficient ν was chosen to be varying along height in accordance with the given $\overline{w'^2}$ profile. In experiments I.10–I.12 it was supposed that $\overline{w'^2} = \overline{w'^2}_{max}$. Calculated in Exp.I.10 ($l = 50$ m) $\overline{u'w'}$ profile is also depicted in Fig.5 by the dashed–dotted line. It is seen from this figure that there are some quantitative differences with case $\nu \not\equiv$ const, but distribution of $\overline{u'w'}$ along height is qualitatively the same. The same picture is true for the other two Exp.'s I.11 and I.12 (figure not shown).

We also conducted the series of experiments III.1–III.3, in which profile of $\overline{w'^2}$ was chosen in form (19), but wind velocity distribution was taken as linear function with gradient $\bar{u}_{max} / H$. Results of calculations for three values of l parameter (50 m in Exp.III.1, 100 m in Exp.III.2 and 200 m in Exp.III.3) are presented in Fig.6. Similar to Figs. 1 and 2 the profile of averaged velocity $\bar{u}$ is also depicted in Fig.6 by the heavy solid line. It is seen from this figure, that although in this series of experiments $\overline{w'^2}$ is varying along height (it means that functions μ and ν are also varying along height) counter–gradient diffusion of momentum is absent.

Winding up the discussion of conducted numerical experiments we can conclude, that a coupled effect of the averaged velocity profile curvature $\partial^2 \bar{u} / \partial z^2$ and the vertical velocity dispersion gradient $\frac{d}{dz}(\overline{w'^2})$ obviously is a main factor, influencing on possibility and character of the formation of the momentum counter–gradient diffusion in jet–like flows.

V. CONCLUSIONS

In this paper results of study of the momentum counter–gradient diffusion in jet–like flows are presented. A simple stationary model based on the 3rd–order–closure scheme has been used to show, that the existence of the momentum counter–gradient diffusion could be explained by the coupled effect of the curvature of averaged wind velocity profile $\partial^2 \bar{u} / \partial z^2$ and gradient of the vertical velocity dispersion $\frac{d}{dz}(\overline{w'^2})$. Depending on sign of this gradient counter–gradient area can form itself above or below the jet axis. The size of this area depends very much on the turbulence length: the more is input of large–scale eddies, the wider is area of the counter–gradient transport. Results of model calculations are in good qualitative agreement with observed atmospheric data (Pennel and LeMone, 1974) and laboratory measurements (Deardorff and Willis, 1987; Narasimha, 1984; Wood and Bradshaw, 1984).

Of course, one can say, thaat vertical scale (H_*) of $\overline{w'^2}$ variability along coordinate z is non arbitrary and must be connected with turbulence scale l. It is possible to show that taking into account such connection we come to the same qualitative conclusions.

Indeed, let us consider an equation of balance for the vertical velocity dispersion (Andre, 1976; Moeng and Randall, 1984; Kurbazkiy, 1988)

$$\frac{d}{dz}(\overline{w'^3}) - (2/3)(C_4 - 1)C_1 l^2 \omega^3 + C_1 C_4 \omega \overline{w'^2} = 0 \ . \tag{22}$$

Taking into account Eq.(8) and notations (12), we can obtain the ordinary differential equation of the 2nd order with respect to $\overline{w'^2}$

$$\frac{d}{dz}\left[v \frac{d}{dz}(\overline{w'^2}) \right] - (2/3)\alpha\omega\overline{w'^2} = -(2/3)\alpha\beta_3 l^2 \omega^3 \ , \tag{23}$$

where $\beta_3 = 2/3(C_4 - 1)/C_4$ (0.52 for $C_4 = 4.5$). If l=const and $e = r\overline{w'^2}$ with $r \equiv$ const, we can obtain an analytical solution of (23), which has for $r < \beta_3^{-1}$ a form (19) of monotonous decreasing along height function with H_* as follows:

$$H_* = \frac{3l}{2(\alpha r(1 - \beta_3 r))^{1/2}} \ . \tag{24}$$

If $r = 3/2$ and l takes consecutively values 50 m, 100 m and 200 m, then formula (24) gives following values of scale H_* : 435 m, 870 m and 1740 m respectively. We have repeated Exp.'s I.1–I.3 with H_* calculated from (24) and found that counter–gradient area existed and placed above jet–axis, but its size was varying much less: 120 m, 160 m and 240 m respectively.

It seems advisable to use the semi–empirical theory developed by Lykossov (1990) for the parameterization of the momentum counter–gradient diffusion in the planetary boundary layer models. It could be realized, for example, by taking into account together with turbulent kinetic energy equation also equations of type (11) for the transport of both zonal and meridional components of momentum. As first guess we can assume a similarity of $\overline{w'^2}$ and turbulent energy e profiles. A following step could be the use of $\overline{w'^2}$ balance equation. Such generalization of semi–empirical theory of the planetary boundary layer does not essentially complicate also its parameterization scheme in large–scal circulation models.

I gratefully acknowledge Prof. R. Narasimha, who has attracted my attention to the problem under consideration, for the personal conversations and useful discussions. I am also indebted to Dr. Ph. Bougeault, Prof. V. P. Dymnikov and Prof. M. Sankar–Rao for the useful comments. This research has been conducted under INDO–USSR Integrated Long Term Programme.

REFERENCES

Andre, J.–C. (1976). A third–order–closure model for the evolution of a convective planetary boundary layer. In: *Seminars on the treatment of the boundary layer in numerical weather prediction*. Reading, 6–10 September 1976, 205–233.

Byzova, N.L., Ivanov, V. N and Garger, E. K.(1989), *Turbulence in atmospheric boundary layer*, Leningrad, Gidrometeoizdat, 264 pp. (in Russian).

Gutman, L. N. (1969). *Introduction into non–linear theory of mesoscale processes*, Leningrad, Gidrometeoizdat, 295 pp. (in Russian).

Das, P. K. (1986), *Monsoons*, Fifth WMO Lecture. –WMO, No.613, Geneva, 155 pp.

Deardorff, J. W., Willis, G. E. (1987), Turbulence within a baroclinic laboratory mixed layer above a sloping surface, *J. Atmos. Sci.*, **44:** 772–778.

Kolmogorff, A. N. (1942). Equations of turbulent motion of non–compressible fluid, *Izvestia ANSSSR*, Ser. fizicheskaya, **6:** 56–58 (in Russian).

Kurbazkiy, A. F. (1988), *Modelling of non–local turbulent transport of impulse and heat*, Novosibirsk, Nauka, 240 pp. (in Russian).

Lykossov, V. N. (1990), K–theory of atmospheric turbulent planetary boundary layer and the Boussinesq's generalized hypothesis, *Sov. j. Numer. Anal. Math. Modelling*, No.3, 221–240.

Marchuk, G. I. (1980), *Methods of numerical mathematics*, Moscow, Nauka, 535 pp. (in Russian).

Milliontschikov, M. D. (1941), On theory of isotropic turbulence, *Doklady Akademii Nauk*, **32:** No.9 611–614.

Moeng, G. H. and Randall, D. A. (1984), Problems in simulating the strato–cumulus–topped boundary layer with a third–order–closure model, *J. Atmos. Sci.*, **41:** 1588–1600.

Narasimha, R. (1984), The turbulence problem: a survey of simple turbulent flows, GALCIT Report FM84–01, Grad. Aero. Lab., California Inst. of Technology, Pasadena, USA, 68 pp.

Pennel, W. T. and LeMone, M. A. (1974), An experimental study of turbulent structure in the fair–weather trade wind boundary layer, *J. Atmos. Sci.*, **31:** 1308–1323.

Rotta, J. C. (1951), Statistische Theorie Nichthomogener Turbulenz, *I. Zs. Phys.*, B. **129:** 547–572.

Speranskiy, L. S., Lykossov, V. N. and Gutman, L. N. (1974), The turbulent planetary boundary layer over curved underlying surface in presence of horizontal heat advection. Izvestia ANSSSR, Serie fizika atmosfery i okeana, **11:** 435–445 (in Russian).

Wood, D. H. and Bradshaw, P. A. (1984), Turbulent mixing layer constrained by a solid surface. Part 2. Measurements in the wall–bounded flow. –*J. Fluid Mech.* **139:** 347–361.